DRUG DEVELOPMENT RESEARCH 66:93–102 (2006)

DDR

Research Article

Mapping the Locations of Estradiol and Potent Neuroprotective Analogues in Phospholipid Bilayers by REDOR

Lynette Cegelski,[1] Charles V. Rice,[1] Robert D. O'Connor,[1] Amy L. Caruano,[2] Gregory P. Tochtrop,[2] Zu Yun Cai,[2] Douglas F. Covey,[2]* and Jacob Schaefer[1]

[1]*Department of Chemistry, Washington University, St. Louis, Missouri*

[2]*Department of Molecular Biology and Pharmacology, Washington University School of Medicine, St. Louis, Missouri*

Strategy, Management and Health Policy				
Enabling Technology, Genomics, Proteomics	Preclinical Research	Preclinical Development Toxicology, Formulation Drug Delivery, Pharmacokinetics	Clinical Development Phases I-III Regulatory, Quality, Manufacturing	Postmarketing Phase IV

ABSTRACT Estrogens are potent antioxidants and neuroprotectants. They have become the focus of drug development efforts aimed at treating and preventing neuronal damage in stroke-related brain damage, Alzheimer's disease, and Parkinson's disease. $^{13}C\{^{31}P\}$ and $^{13}C\{^{19}F\}$ rotational-echo double-resonance NMR have been used to map the locations of 17β-estradiol (estradiol), 17β-estradiol 17-benzoate (estradiol benzoate), and 17β-2-(1-adamantyl)estradiol (adamantyl estradiol) in ^{19}F-labeled DPPC phospholipid multilamellar vesicles. Placement of the estrogen molecules in lipid bilayers is correlated with the differences in their neuroprotective potency. Drug Dev. Res. 66:93–102, 2006.

Key words: solid-state NMR; estrogens; neuroprotection; membranes; REDOR; lipid bilayers

INTRODUCTION

17β-Estradiol (hereafter "estradiol") is the most physiologically active of the three naturally-produced estrogens that influence the development of secondary sexual characteristics in females. Estrogen-containing pharmaceuticals are widely prescribed in the scope of estrogen's natural hormonal roles, e.g., in postmenopausal estrogen therapy as well as in birth-control formulations. Estrogens are also equipped to prevent cell damage and cell lysis by scavenging free radicals within the bilayer [Barclay, 1993]. The free-radical scavenging property of estradiol has been attributed to its ability to quench lipid hydroperoxy radicals by donation of the hydrogen atom from the hydroxyl group of the phenyl ring, whose aromatic nature stabilizes the resulting oxygen radical [Lacort et al., 1995; Kagan et al., 1990]. In fact, the minimal structural elements required for neuroprotection by estradiol have been identified as the hydroxyl group on the steroid A-ring and planarity of the steroid ring backbone [Dykens et al., 2004; Pike, 1999; Nakamizo et al., 2000; Green et al., 1997, 2001]. Therefore,

Grant sponsor: NIH; Grant numbers: EB 002058; AG 10485; 5 T32 GM 08785; Grant sponsor: Apollo Biopharmceutics, Inc.

Charles V. Rice's present address is Department of Chemistry and Biochemistry, The University of Oklahoma, Norman, OK 73019.

Robert D. O'Connor's present address is Department of Radiology/Mallinckrodt Institute of Radiology, Washington University School of Medicine, St. Louis, MO 63110.

Gregory P. Tochtrop's present address is Department of Chemistry and Chemical Biology, Harvard University, Cambridge, MA 02138.

*Correspondence to: Douglas F. Covey, Department of Molecular Biology and Pharmacology, Washington University School of Medicine, Campus Box 8103, 660 South Euclid Avenue, St. Louis, MO 63110. E-mail: dcovey@wustl.edu

Published online in Wiley InterScience (www.interscience.wiley.com). DOI: 10.1002/ddr.20048

estrogens are the focus of an increasing number of therapeutic strategies aimed at alleviating and preventing the devastating consequences of cellular injury implicated in neurodegenerative diseases, including stroke-related brain damage, Alzheimer's disease, Parkinson's disease, glaucoma, and retinitis pigmentosa [Gordon et al., 2005; Simpkins et al., 2005; Wise et al., 2000; Behl and Manthey, 2000; Garcia-Segura et al., 2001]. However, the therapeutic use of estradiol for treatment of neurological diseases is compromised by the undesirable side-effects of a global increase of feminizing hormone levels in the body.

The estrogen analogue, adamantyl estradiol, belongs to an attractive class of molecules that mediates neuroprotection without binding to estrogen receptors [Perez et al., 2006]. These estradiol analogues lack the hormonal properties that hinder the therapeutic utility of estrogen as a neuroprotectant. In particular, adamantyl estradiol, also known as ZYC-5 and MX-4565, was demonstrated to lack activity at the classical estrogen receptor, and to provide more robust protection of cortical neurons from death induced by N-methyl-D-aspartate (NMDA) than estradiol [Xia et al., 2002]. Other adamantyl substituted estrogen analogues also have enhanced neuroprotective actions in a variety of in vivo and cell culture models of neuronal cell death [Liu et al., 2002; Simpkins et al., 2004; Kumar et al., 2005; Perez et al., 2005a; Dykens et al., 2004]. Adamantyl estradiol is a more effective free radical scavenger than estradiol [Perez et al., 2005], accounting in part for its enhanced neuroprotective actions, although additional factors likely also contribute to the mechanism of action.

Rotational-echo double-resonance (REDOR) NMR provides a direct measure of short- and long-range dipolar couplings between isolated pairs of labeled nuclei [Gullion and Schaefer, 1989a,b]. The couplings contain information on both internuclear distances and orientations [O'Connor and Schaefer, 2002] so that REDOR is both a spectroscopic ruler and protractor. The REDOR strategy is generally not one of total-structure determination, but rather one of accessing site-specific atomic-level information to yield facts and structural restraints that may help characterize function in systems as complex as bacterial whole cells and intact plant leaves [Tong et al., 1997; Cegelski et al., 2002; Cegelski and Schaefer, 2005]. REDOR has recently been applied extensively to studies of native-state and perturbed lipid bilayers; e.g., those disrupted by the action of magainin antimicrobial peptides [Toke et al., 2004a,b].

In this report, the mapping of three different sterols in the lipid environment was undertaken to help provide insight into the biological properties of the molecules. Estradiol has been established as a lipid antioxidant and neuroprotectant [Mooradian, 1993; Romer et al., 1997a,b; Miller et al., 1996]. Estradiol benzoate exhibits reduced neuroprotective potency against glutamate cell killing as compared to estradiol, but adamantyl estradiol provides enhanced neuroprotection [Perez et al., 2006 (this issue); Xia et al., 2002]. Here we identify the spatial preferences that these three sterols have in the phospholipid bilayer. The differential spatial partitioning of these sterols may yield insights into their capacity to scavenge free radicals and so prevent oxidative damage. Our ultimate goal is to provide a biophysical rationale for some of the structure–activity relationships observed for sterols with different structural modifications.

MATERIALS AND METHODS

Lipids

^{19}F-labeled dipalmitoylphosphadityl choline (F-DPPC) was synthesized from 16-fluoropalmitic acid [Toke et al., 2004b] by Avanti Polar Lipids, Inc. (Alabaster, AL). F-DPPC and DPPC were used as supplied from Avanti Polar Lipids, Inc. The purity of these compounds was confirmed by thin-layer chromatography.

Synthesis of ^{13}C Labeled Estradiol and Its Derivatives

The [3-^{13}C]estradiol was prepared from 19-nortestosterone (Steraloids, Inc.) using the method reported by [Yuan 1982] for the preparation of [3,4-$^{13}C_2$]estradiol except that [1-^{13}C]-acetyl chloride (Cambridge Isotope Laboratories, Inc.) was used in place of [1,2-$^{13}C_2$]-acetyl chloride. The [3-^{13}C]estradiol benzoate was prepared from [3-^{13}C]-19-nortestosterone benzoate (an intermediate in the preparation of the [3-^{13}C]estradiol) using the aromatization procedure of Rao et al. [1994]. The adamantyl [3-^{13}C]estradiol was prepared by reacting [3-^{13}C]estradiol with 1-adamantanol according to the method of Lunn and Farkas [1968]. The estradiol [1-^{13}C]benzoate was prepared from estrone by: (1) benzylation of the 3-hydroxyl group of estrone, (2) reduction of the 17-ketone of estrone to the 17β-hydroxyl group, (3) esterification of the 17β-hydroxyl group with [1-^{13}C]-benzoic acid (Isotec, Inc.), and (4) removal of the 3-benzyl group by hydrogenolysis.

Sterols in Multi-Lamellar Vesicles (MLVs)

^{13}C-labeled sterols were embedded in DPPC multi-lamellar vesicles (MLVs) by the following procedure. Using a pear-shaped flask, 15 μmol sterol was dissolved in 1 ml methylene chloride. A solution of 4 ml methylene chloride, 1 ml chloroform, and 300 μmol of lipid (15 μmol ^{19}F-DPPC and 285 μmol DPPC) were added and gently mixed with a vortex mixer. After

heating to 37°C, the solvent was removed using a stream of dry nitrogen. The residue was resuspended in 2 ml degassed aqueous buffer (20 mM PIPES/1 mM EDTA, pH 7.0) and mixed with a vortex mixer. The flask was placed in a 65°C water bath for 10 min, vortexed vigorously, and placed in a dry ice/ethanol bath for 10 min. The heating and cooling cycle was repeated three additional times. A nitrogen atmosphere over the sample was maintained at all times. After the last cooling step, the sample vial was cooled in liquid nitrogen and lyophilized. It is known from REDOR experiments that the state of MLVs is similar for gel state, frozen, and lyophilized samples [Hirsh et al., 1996; Toke et al., 2004a,b].

Rotational-Echo Double Resonance

REDOR was used to restore the dipolar couplings between heteronuclear pairs of spins that are removed by magic-angle spinning [Gullion and Schaefer, 1989a,b]. REDOR experiments are always done in two parts, once with rotor-synchronized dephasing pulses (S) and once without (S_0). The dephasing pulses change the sign of the heteronuclear dipolar coupling, and this interferes with the spatial averaging resulting from the motion of the rotor. The difference in signal intensity ($\Delta S = S_0 - S$) for the observed spin in the two parts of the REDOR experiment is directly related to the corresponding distance to the dephasing spin. REDOR has found application in the characterization of binding sites of proteins [McDowell and Schaefer, 1996; McDowell et al., 2003, 2004] and in the analysis of heterogeneous biological materials such as amyloid plaques [Balbach et al., 2000], membrane protein helical bundles [Smith et al., 2001], and bacterial cell walls [Cegelski et al., 2002; Kim et al., 2002].

Spectrometer

REDOR NMR was performed using a 6-frequency transmission-line probe [Schaefer and McKay, 1999] having a 12-mm-long, 6-mm inside-diameter analytical coil and a Chemagnetics/Varian ceramic stator. Lyophilized samples were contained in thin-wall Chemagnetics/Varian 5-mm outside-diameter zirconia rotors. The rotors were spun at 7143 Hz with the speed under active control to within ± 2 Hz. A stack-mounted air chiller cooled the rotor to an exit-gas temperature of -20°C. The spectrometer was controlled by a Tecmag pulse programmer. Radio-frequency pulses for ^{31}P (202 MHz) and ^{13}C (125 MHz) were produced by 1- and 2-kW American Microwave Technology power amplifiers, respectively. Proton (500 MHz) and ^{19}F (470 MHz) radio-frequency pulses were generated by 2-kW Amplifier Systems tube amplifiers driven by 50-watt American Microwave Technology power amplifiers. The π-pulse lengths were 6 μsec for ^{31}P, 8 μsec for ^{13}C, and 5.0 μsec for ^{19}F.

^{13}C{^{31}P} and ^{13}C{^{19}F} REDOR spectra were collected with xy-8 phase-cycled π pulses on both observed and dephasing channels [Gullion et al., 1990; Weldeghiorghis and Schaefer, 2003]. A 12-T static magnetic field was provided by an 89-mm bore Magnex superconducting solenoid. Proton-carbon cross-polarization transfers were made in 2 msec with radio-frequency fields of 62.5 kHz. Proton dipolar decoupling was 100 kHz during data acquisition.

RESULTS

Carbon-Phosphorous Contact

Each set of REDOR spectra contains information about lipid–lipid and sterol–lipid contacts. The ^{13}C{^{31}P} REDOR measurement of estradiol-containing MLVs at the short evolution time of 6.72 ms identifies close carbon-phosphorous contacts (Fig. 1, left). The lipid carbonyl carbon peak at 172 ppm is dephased by 31%, which represents an average dephasing for both carbonyl carbons. The labeled estradiol carbon is dephased to the same extent. This places the estradiol carbon at about the same distance from phosphorous as the average of the lipid carbonyl distances. The lipid headgroup ^{13}C{^{31}P} dephasing (60–70 ppm) is nearly 100%, expected for 2–5 Å distances. At this short evolution time, there is no contact for the lipid methyl carbons (14 ppm) and only weak contact for aliphatics near the headgroups (30 ppm).

The extent of ^{31}P dephasing of the lipid carbonyl carbons increases to 82%, and that of the labeled sterol carbon to 81%, at the longer evolution time of 26.88 ms (Fig. 1, right). The headgroup carbons are completely dephased and the lipid aliphatic carbon dephasing has increased. In addition, the lipid tail methyl carbons are now accessible and contribute to the REDOR difference spectrum. The 3% ^{13}C{^{31}P} dephasing represents a distance that is at least 13 Å [Gullion and Schaefer, 1989a,b].

^{13}C{^{31}P} REDOR measurements for MLVs with [3-^{13}C]estradiol benzoate (Fig. 2, left) and estradiol [1-^{13}C]benzoate (Fig. 2, right) reveal that the [3-^{13}C]label, dephased by 57%, is positioned similarly to the lipid carbonyl carbon and is near the lipid headgroups. However, there is no observable dephasing for the 1-^{13}C label, which means that it is far from the lipid headgroups. Figure 3 lists the measured ^{13}C{^{31}P} dephasing for all four samples at the 8.96-ms evolution time, corresponding to 64 rotor cycles. This provides a simple qualitative assessment of the sterol positions

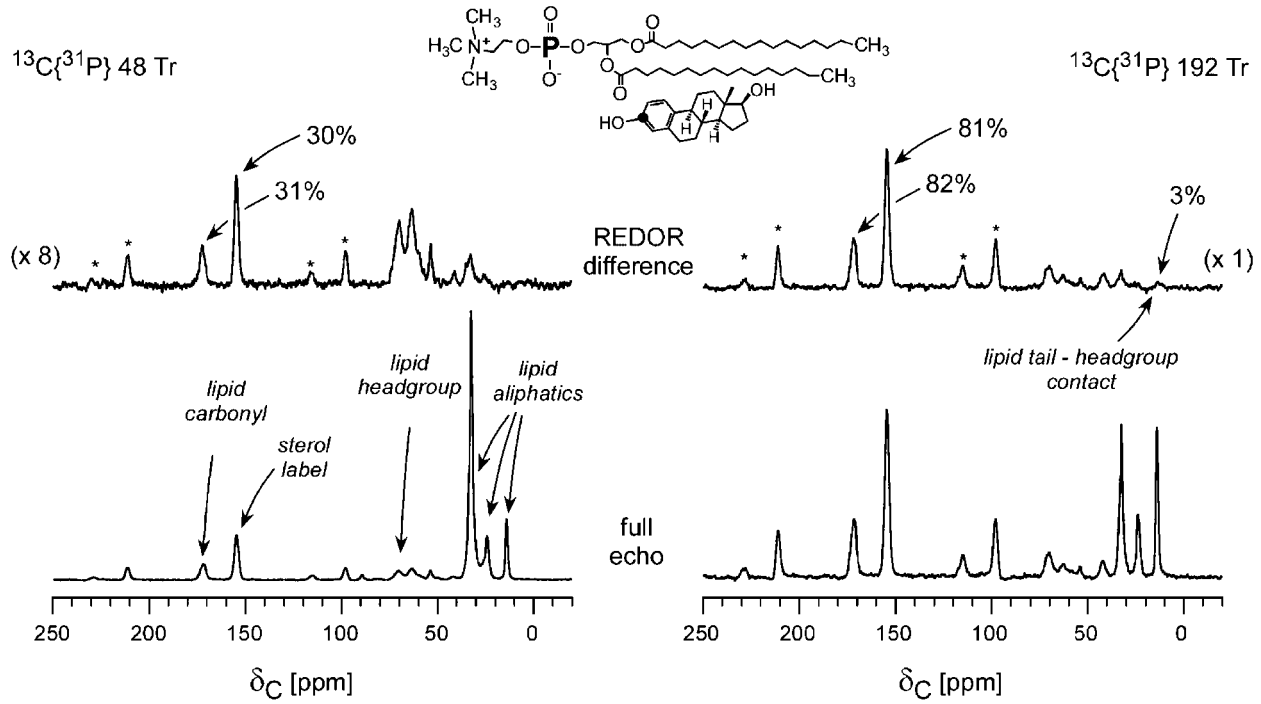

Fig. 1. $^{13}C\{^{31}P\}$ REDOR spectra of [3-^{13}C]estradiol in a lipid bilayer after 48 (6.72 ms) and 192 (26.88 ms) rotor cycles of dipolar evolution. The full-echo spectra are shown at the bottom of the figure and the REDOR difference spectra at the top. Dephasing for the peak due to the sterol label (solid circle, inset) is comparable to that for the lipid carbonyl-carbon peak for both evolution times. Magic-angle spinning was at 7,143 Hz. Prominent spinning sidebands are marked by asterisks.

in the lipid bilayer. The $^{13}C\{^{31}P\}$ results reveal that the three 3-^{13}C labels are near the headgroup and the 1-^{13}C label of estradiol benzoate is far from the headgroup.

A more detailed assessment of sterol placement in the bilayer is only possible through a full analysis of REDOR dephasing as a function of time. The curves in Figure 4 compare the $^{13}C\{^{31}P\}$ dephasing of the three 3-^{13}C sterol labels with that of the lipid carbonyl carbons. The differences in the initial slopes and overall rates of increase of the dephasing curves reveal the proximities of the labeled sterol carbons and lipid carbonyl carbons relative to the phosphate headgroup. The estradiol benzoate label (stars) is closest, followed by that of the lipid carbonyl carbons, estradiol, and adamantyl estradiol labels. The biphasic nature of the dephasing curve for estradiol benzoate (dashed line) suggests that there is a distribution of distances from the [3-^{13}C]estradiol benzoate carbon to phosphorous. At least one distance is shorter than that for the carbonyl carbons so that the dephasing grows in quickly and plateaus, and one or more distances are longer and result in the later rise in dephasing after 20 ms. The steep initial slope of the adamantyl [3-^{13}C]estradiol dephasing indicates a phosphorous proximity that is nearer than that for the carbonyls. However, the dephasing slows and does not continue to increase as fast as the dephasing for the lipid carbonyls with increasing dipolar evolution time. This behavior indicates a second population of adamantyl estradiol molecules that is farther away from ^{31}P than the distribution of lipid carbonyls. Qualitatively, this could be either a sizable population that is slightly more distant, or a smaller population that is much more distant from the ^{31}P atoms.

Carbon-Fluorine Contact

$^{13}C\{^{19}F\}$ REDOR measurements identify proximities to the lipid core. Figure 5 compares the $^{13}C\{^{19}F\}$ REDOR spectra of MLVs without (Fig. 5, left) and with sterol (Fig. 5, right). Dephasing for the MLV sample with no sterols identifies the proximities to the fluorine of the lipid aliphatics. When sterols are added, the lipid dephasing profile remains approximately the same. The aliphatic carbon-chain dephasing was similar for all sterol preparations (only the estradiol spectra are presented here). The methyl carbons also dephase similarly for all preparations, with $\Delta S/S_0$ values between 24 and 28%. The minor differences are probably the result of slight variations in packing

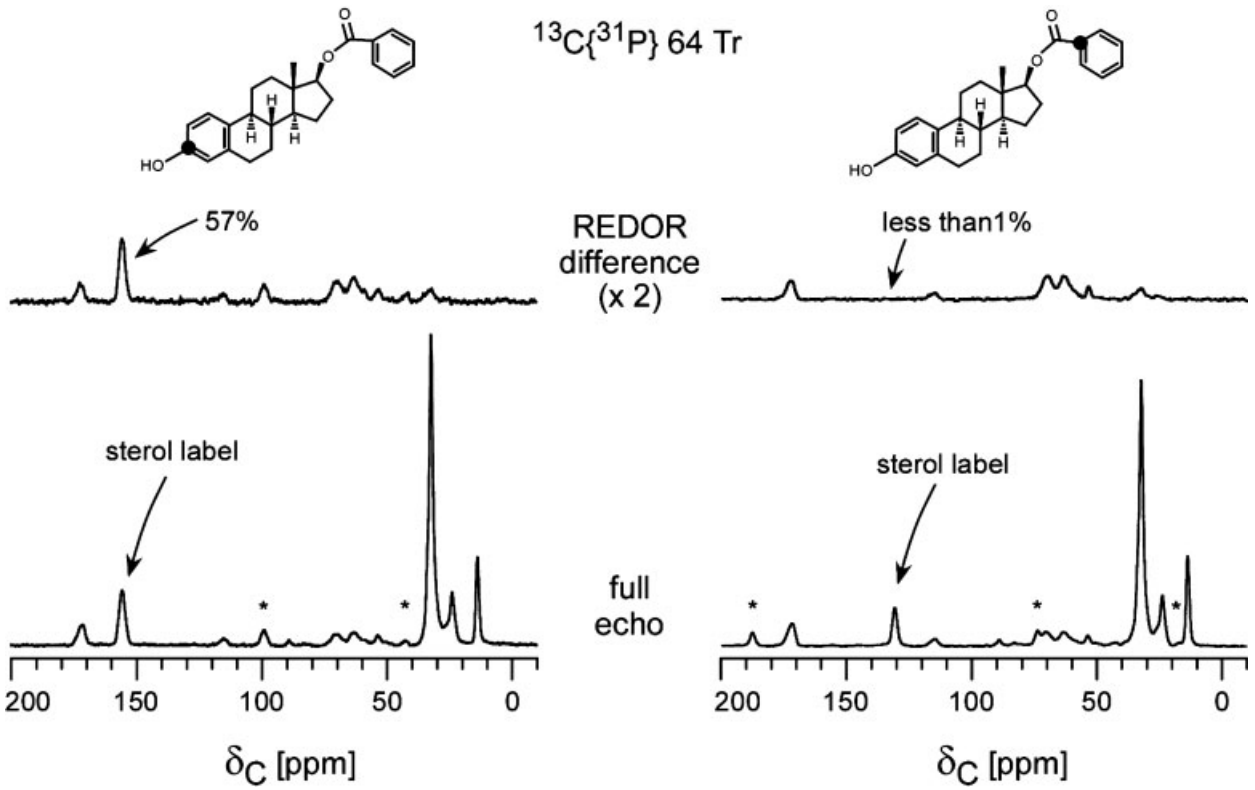

Fig. 2. $^{13}C\{^{31}P\}$ REDOR spectra of [3-^{13}C]estradiol benzoate (left) and estradiol [1-^{13}C]benzoate (right) in a lipid bilayer after 64 rotor cycles (8.96 ms) of dipolar evolution. The full-echo spectra are shown at the bottom of the figure and the REDOR difference spectra at the top. The absence of observable dephasing for the peak due to the label in the benzoate ring (solid circle, inset, right) places that labeled carbon distant from the lipid headgroups. Magic-angle spinning was at 7,143 Hz. Spinning sidebands of peaks corresponding to the sterol labeled carbons are marked by asterisks.

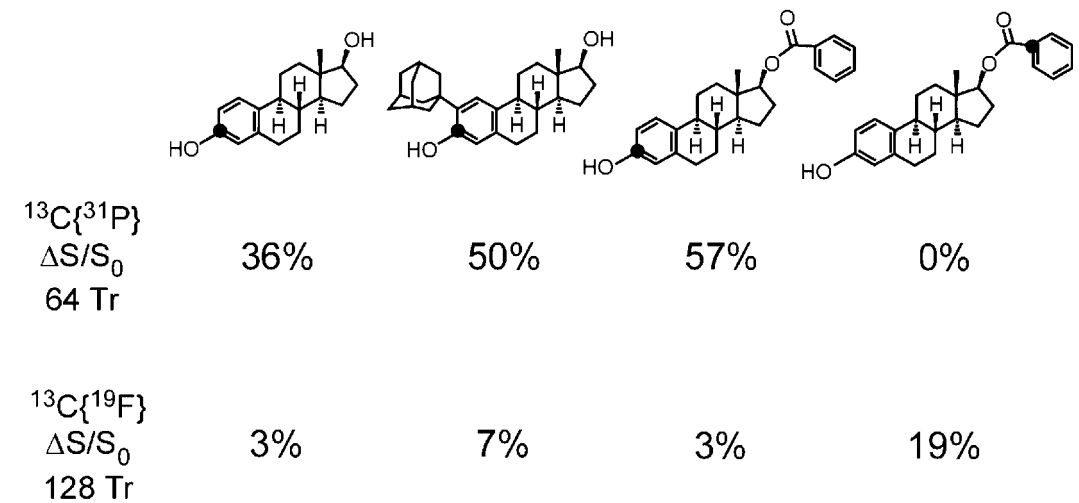

Fig. 3. Selected values of REDOR dephasing for the labeled carbons (solid circles) of (left to right) [3-^{13}C]estradiol, adamantyl [3-^{13}C]estradiol, [3-^{13}C]estradiol benzoate, and estradiol [1-^{13}C]benzoate. For estradiol benzoate, both $^{13}C\{^{31}P\}$ and $^{13}C\{^{19}F\}$ dephasing of the peaks corresponding to the two labels unambiguously place the hydroxyl substituent near the lipid headgroups, and the benzoate moiety near the lipid tails.

for the sterol-lipids. The 3-^{13}C estradiol label is coupled weakly to the fluorinated tails, and yields only 3% dephasing after 17.92 ms of dipolar evolution (Fig. 5, right). The 3-^{13}C labels of the two other sterols are also distant from the tails, consistent with their proximity to phosphorous (see Fig. 3, bottom row).

Figure 6 provides a comparison of $^{13}C\{^{19}F\}$ REDOR spectra for the two labeled estradiol benzoates. The 3-^{13}C label has weak dephasing and so is distant from fluorine, whereas the [1-^{13}C]benzoate label yields 19% dephasing and is, therefore, close to fluorine. Comparison of the $^{13}C\{^{19}F\}$ and $^{13}C\{^{31}P\}$ dephasing for the 1-^{13}C and 3-^{13}C labeled-carbon peaks of estradiol benzoate (Figs. 2 and 6) unambiguously demonstrates that the sterol orients in the bilayer with the 3-^{13}C label near the ^{31}P headgroup and the [1-^{13}C]benzoate label near the lipid tails.

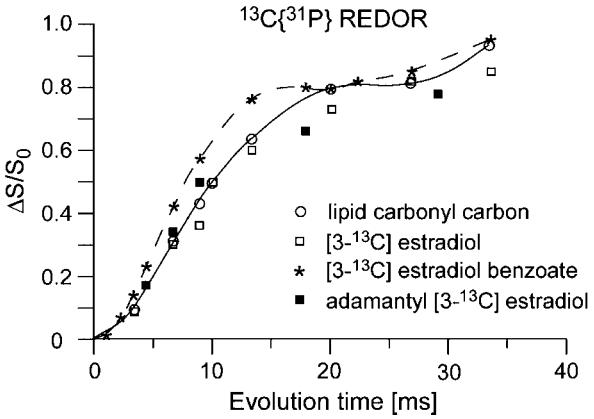

Fig. 4. Dependence of the $^{13}C\{^{31}P\}$ dephasing ($\Delta S/S_0$) on dipolar evolution time for the labeled-carbon peaks of three sterols in lipid bilayers, and for the natural-abundance ^{13}C peak of the lipid carbonyl carbons. The dashed line highlights qualitatively the dephasing for the labeled-carbon peak of [3-^{13}C]estradiol benzoate, and the solid line indicates the dephasing for the lipid carbonyl-carbon peak. Both lines suggest the presence of two populations with differing dephasing behavior. Based on signal-to-noise ratios, the errors in the dephasing values are within the heights of the symbols.

In contrast to the $^{13}C\{^{31}P\}$ REDOR measurements where 100% of the headgroups have ^{31}P dephasers, only 5% of the DPPC lipid tails are singly fluorinated. This creates a lipid environment around the sterol where a ^{13}C-^{19}F isolated-pair approximation may be used to determine average carbon-fluorine proximities [O'Connor and Schaefer, 2002; Toke et al., 2004b]. Thus, a full REDOR curve was calculated for estradiol [1-^{13}C]benzoate MLVs assuming a Gaussian distribution of carbon-fluorine distances (Fig. 7). Calculated dephasing (solid line) and experimental dephasing (circles) match for evolution times between 2 and 28 msec. The average ^{13}C-^{19}F distance is 14 Å (Fig. 7, inset).

DISCUSSION

REDOR Cartography

REDOR measurements are often used to measure exact distances between isolated pairs of NMR labels. In the lipid bilayer, however, phosphate headgroups create a system where there are multiple ^{31}P dephasers. Distance measurements with multiple dephasers are model dependent, and for bilayers require knowledge of the lipid areas (to yield the

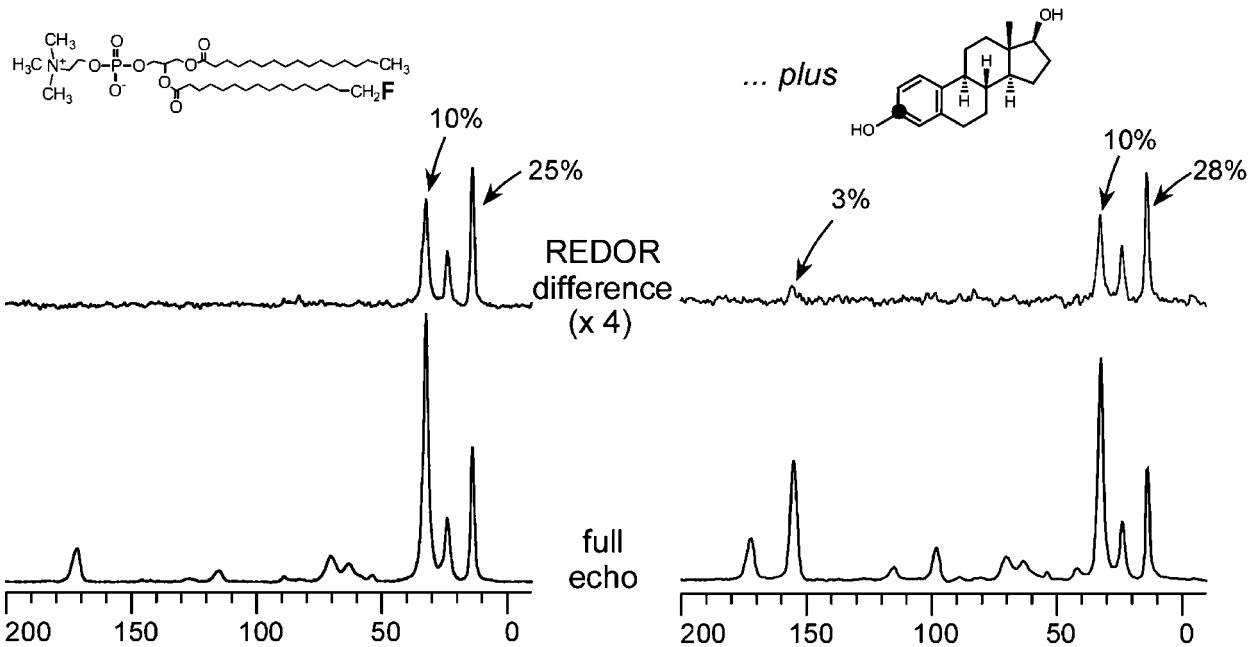

Fig. 5. $^{13}C\{^{19}F\}$ REDOR spectra of a lipid bilayer containing 5% fluorinated DPPC and 95% DPPC (left) and of the same bilayer with [3-^{13}C]estradiol (right) after 128 rotor cycles (17.92 ms) of dipolar evolution. The full-echo spectra are shown at the bottom of the figure and the REDOR difference spectra at the top. Magic-angle spinning was at 7,143 Hz.

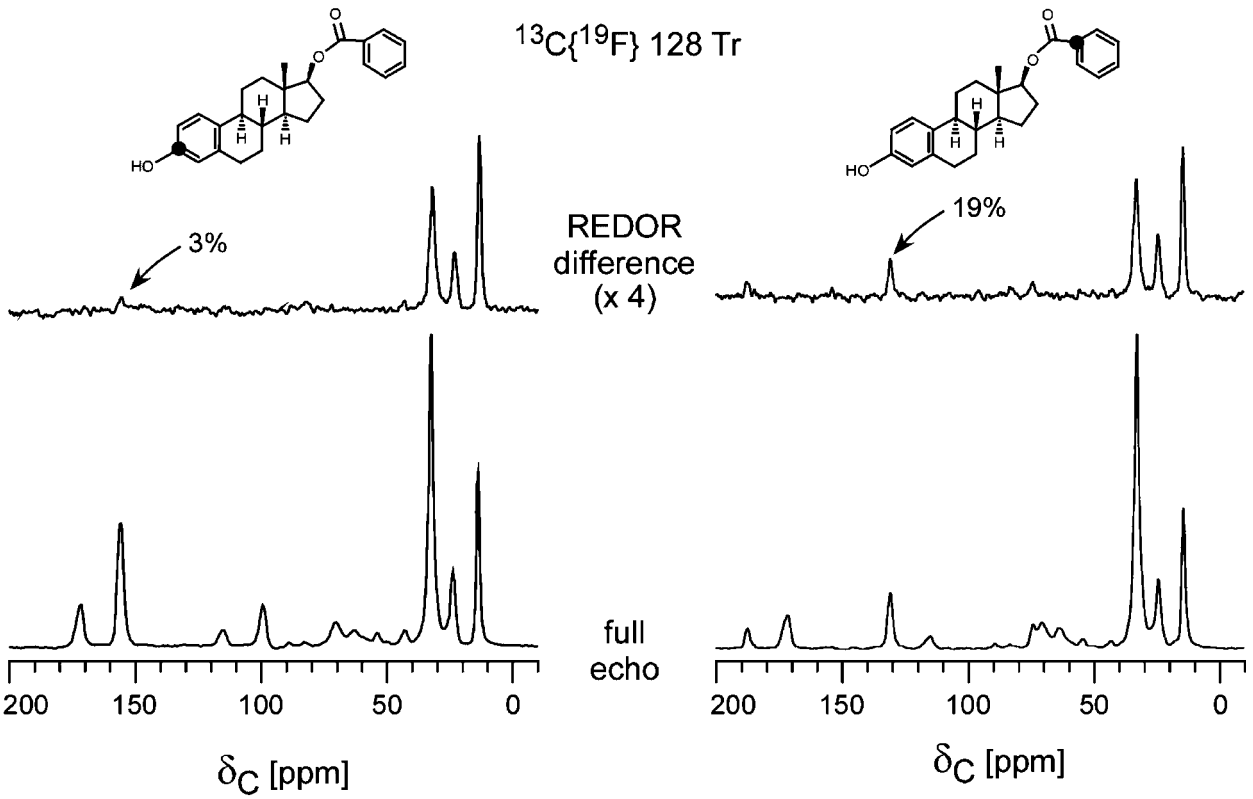

Fig. 6. $^{13}C\{^{19}F\}$ REDOR spectra of a lipid bilayer containing 5% fluorinated DPPC and 95% DPPC with [3-^{13}C]estradiol benzoate (left) and estradiol [1-^{13}C]benzoate (right) after 128 rotor cycles (17.92 ms) of dipolar evolution. The full-echo spectra are shown at the bottom of the figure and the REDOR difference spectra at the top. The substantial dephasing for the peak due to the label in the benzoate ring (solid circle, inset, right) places that labeled carbon proximate to the lipid tails. Magic-angle spinning was at 7,143 Hz.

spacing of the ^{31}P atoms), as well as of the orientation of ^{13}C-^{31}P dipolar tensors. For the sterol-lipids of Figure 3, a much simpler strategy has been adopted that is akin to geographical cartography. We use the REDOR dephasing by ^{31}P at one end of the lipid chain, and by ^{19}F at the other, to map the sterols in the phospholipid bilayer with respect to lipid atomic landmarks. The landmarks are the headgroup carbons, the carbonyl carbons, and the methyl tails. In effect, these landmarks define lines of latitude in the lipid bilayer. We then compare the REDOR dephasing of the guest sterol with that of landmarks to map the relative locations of sterol and landmarks.

The spectra in Figure 1 illustrate the mapping strategy for [3-^{13}C]estradiol. The dipolar coupling, which is measured in REDOR, evolves as a function of time. This means that, at short evolution times, the REDOR measurement serves as a short-range ruler, identifying only carbons that are near phosphorous (Fig. 1, left). Thus, the lipid methyl carbons are out of range of the phosphate headgroups for short evolution times and no REDOR dephasing is observed for these carbons. But the methyl carbons are monitored with the longer range detection afforded by a longer dipolar evolution time (Fig. 1, right). Because the label of [3-^{13}C]estradiol has a $^{13}C\{^{31}P\}$ REDOR difference comparable to that of the lipid carbonyl carbons, the sterol label must be in the same vicinity as the lipid carbonyl-carbon landmark.

Figure 3 provides a snapshot of REDOR dephasing for particular evolution times for all the sterols. These data summarize the qualitative placement of the sterols in the lipid bilayer. Based on the relative $^{13}C\{^{31}P\}$ dephasing, the three 3-^{13}C sterol labels are all near the lipid headgroups, and the estradiol [1-^{13}C]benzoate label is remote. The sterol-lipid-tail contacts, measured by $^{13}C\{^{19}F\}$ REDOR, confirm that the 3-^{13}C labels are indeed far from the lipid tails (not much dephasing), while the benzoate moiety is near the tails (sizeable dephasing). The combination of $^{13}C\{^{31}P\}$ and $^{13}C\{^{19}F\}$ dephasing for the estradiol benzoate labels is consistent with the span of the bilayer: the 1-^{13}C label is about 14 Å from the lipid tail (Fig. 7) and 12 Å from the 3-^{13}C label on the other end of the rigid framework of the molecule, which is itself just a few Å from the ^{31}P of the head group. These distances combined account for 28 Å between lipid head group and tail, a little more than the

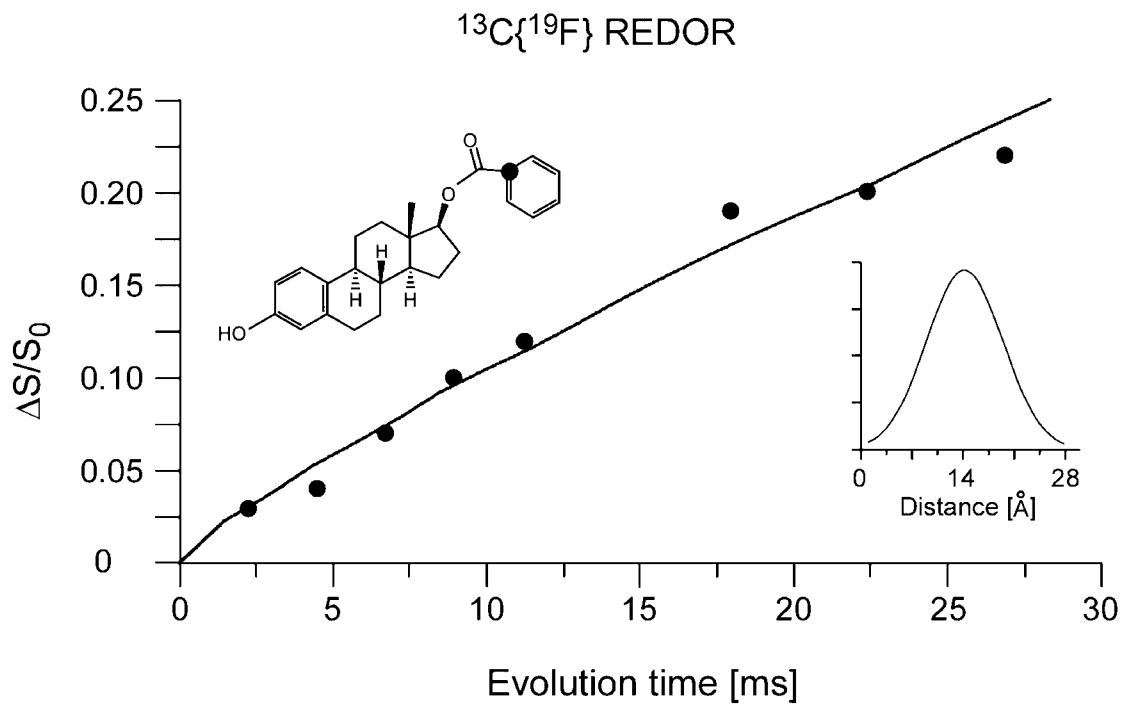

Fig. 7. Dependence of the $^{13}C\{^{19}F\}$ dephasing ($\Delta S/S_0$) on dipolar evolution time for the labeled-carbon peak of estradiol [1-^{13}C]benzoate. The solid line is the calculated dephasing for a Gaussian distribution (inset, right) of isolated ^{13}C-^{19}F distances. The distribution arises from a random placement of the ^{19}F label in the tails of lipid chains within dipolar contact of the labeled carbon [Toke et al., 2004a].

accepted value for gel-phase DPPC bilayers of 22–24 Å [Tristram-Nagle and Nagle, 2004]. The discrepancy suggests that estradiol benzoate is probably tilted within the bilayer.

Multiple Sterol Populations

Unlike X-ray crystallography and solid-state NMR total-structure determinations [Straus et al., 1997; Pauli et al., 2000], which require uniform packing and identical atomic coordinates over the entire sample, REDOR NMR does not demand sample homogeneity. The $^{13}C\{^{31}P\}$ REDOR curves in Figure 4, in fact, reflect the existence of distance distributions in the bilayers. For example, the two-plateau dephasing observed for the lipid carbonyl carbons (solid line) is typical of a multi-distance distribution [O'Connor et al., 2002], corresponding to different distances for each of the two carbonyl carbons to the head groups. The two-plateau dephasing of [3-^{13}C]estradiol benzoate (Fig. 4, dashed line) indicates at least two populations in the bilayer, one of which places the label closer to the lipid headgroups on average than the carbonyl carbons, and the other that brings the 3-^{13}C label within fluorine dephasing range.

The sizeable $^{13}C\{^{31}P\}$ dephasing *and* $^{13}C\{^{19}F\}$ dephasing for adamantyl estradiol (Fig. 3) also suggests that there is a population of sterols closer to phosphorous than the average lipid carbonyl carbons, and, at the same time, a population that is near the fluorine tails. Figure 8 (extreme right) illustrates schematically a pair of sterols consistent with the observed dephasing. If a population of adamantyl estradiols were flipped from the usual upright estradiol orientation (possibly the result of aggregation or the adamantyl-induced hydrophobicity of the hydroxyl ring), the free-radical scavenging hydroxyl group would be closer to the unsaturated carbons present in mammalian lipid bilayers. However, the population of flipped admantyl estradiols is necessarily small because of the significant $^{13}C\{^{31}P\}$ REDOR difference of Figure 3.

These REDOR experiments indicate that structural modification of the estradiol molecule affects both the depth at which the molecule resides in the membrane and its orientation; i.e., which part of the molecule is interacting with the polar headgroups, and which part with the hydrophobic core of the membrane. Of particular interest to drug development efforts are the results showing that the adamantyl group placed at the C-2 position of estradiol produces an analogue that partially orients itself in the membrane bilayer with the phenolic ring toward the center of the membrane bilayer. Such an orientation locates the phenol group near the double bonds of unsaturated fatty acids in membrane lipids. Because these double

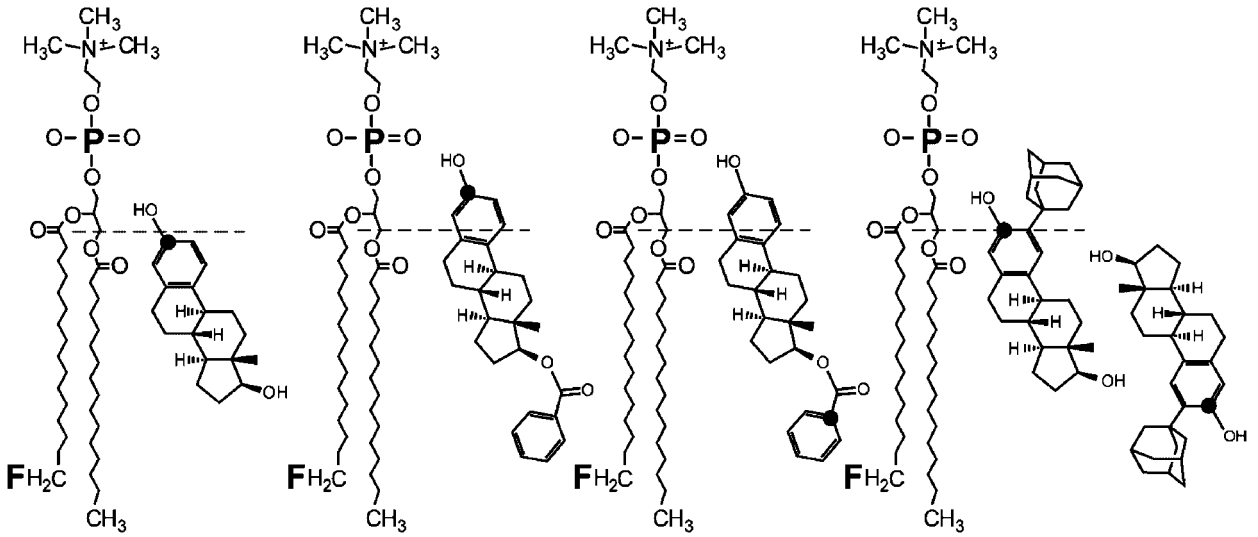

Fig. 8. Schematic representation of the placement of the labeled sterols within a lipid bilayer based on the REDOR results of Figure 4.

bonds are involved in lipid peroxidation reactions, it seems reasonable to conclude that having the free-radical quenching phenol group near the double bonds, instead of near the lipid polar head groups, would lead to better protection against oxidative stress in cells, and, in particular, the mitochondrial inner membrane of cells because of the increased amounts of reactive oxygen species associated with mitochondrial malfunction. Consequently, this orientation effect could contribute to the enhanced neuroprotective effect observed for MX-4565 (ZYC-5) in studies of oxidative stress in cultured HT-22 hippocampal cells [Perez et al., 2006].

It would be of interest in the future to use REDOR to map the locations of other lipid soluble free-radical quenching agents in membrane bilayers and then to correlate their locations with the ability to reduce oxidative stress in cells. Perhaps the increased extent to which the free-radical quenching group of these agents is located proximate to the double bonds of the fatty acids contained in the membrane lipids will correlate with an enhanced ability to prevent damage from oxidative stress in cells. Such a correlation would provide a structural rationale for the development of future drugs capable of preventing and alleviating the cellular injury sustained in many neurodegenerative diseases.

ACKNOWLEDGMENTS

This work was supported in part by NIH grants EB 002058 (J.S.), AG 10485 (D.F.C.), NIH training grant 5 T32 GM 08785 (L.C.), and a research grant to D.F.C. from Apollo Biopharmceutics, Inc., prior to its acquisition by MIGENIX Corp.

REFERENCES

Balbach JJ, Ishii Y, Antzutkin ON, Leapman RD, Rizz NW, Dyda F, Reed J, Tycko R. 2000. Amyloid fibril formation by Aβ16-22, a seven-residue fragment of the Alzheimer's β-amyloid peptide, and structural characterization by solid state NMR. Biochemistry 39: 13748–13759.

Barclay LRC. 1993. Model biomembranes: quantitative studies of peroxidation, antioxidant action, partitioning, and oxidative stress. Can J Chem 71:1–16.

Behl C, Manthey D. 2000. Neuroprotective activities of estrogen: an update. J Neurocytol 29:351–359.

Cegelski L, Kim SJ, Hing AW, Studelska DR, O'Connor, RD, Mehta AK, Schaefer J. 2002. Rotational-echo double resonance characterization of the effects of vancomycin on cell wall synthesis in *Staphylococcus aureus*. Biochemistry 41:13053–13058.

Cegelski L, Schaefer J. 2005. Glycine metabolism in intact leaves by in vivo ^{13}C and ^{15}N labeling. J Biol Chem 280:39238–39245.

Dykens JA, Caroll AK, Wiley S, Covey DF, Cai ZY, Zhao L, Wen R. 2004. Photoreceptor preservation in the S334ter model of retinitis pigmentosa by a novel estradiol analog. Biochem Pharmacol 68: 1971–1984.

Garcia-Segura LM, Azcoitia I, DonCarlos LL. 2001. Neuroprotection by estradiol. Prog Neurobiol 63:29–60.

Gordon KB, Macrae IM, Carswell HVO. 2005. Effects of 17β-oestradiol on cerebral ischaemic damage and lipid peroxidation. Brain Res 1036:155–162.

Green PS, Gordon K, Simpkins JW. 1997. Phenolic A ring requirement for the neuroprotective effects of steroids. J Steroid Biochem Mol Biol 63:229–235.

Green PS, Yang SH, Nilsson KR, Kumar AS, Covey DF, Simpkins JW. 2001. The nonfeminizing enantiomer of 17β-estradiol exerts protective effects in neuronal cultures and a rat model of cerebral ischemia. Endocrinology 142:400–406.

Gullion T, Schaefer J. 1989a. Detection of weak heteronuclear dipolar couplings by rotational-echo double-resonance nuclear magnetic resonance. In: Advances in magnetic resonance. New York: Academic Press. p 57–83.

Gullion T, Schaefer J. 1989b. Rotational-echo double-resonance NMR. J Magn Reson 81:196–200.

Gullion T, Baker DB, Conradi MS. 1990. New, compensated Carr-Purcell sequences. J Magn Reson 89:479–484.

Hirsh D, Hammer J, Maloy JW, Blazyk J, Schaefer J. 1996. Secondary structure and location of a magainin analogue in synthetic phospholipid bilayers. Biochemistry 35:12733–12741.

Kagan VE, Serbinova EA, Bakalova RA, Stoytchev TS, Erin AN, Prilipko LL, Evstigneeva RP. 1990. Mechanisms of stabilization of biomembranes by α-tocopherol: the role of the hydrocarbon chain in the inhibition of lipid-peroxidation. Biochem Pharmacol 40:2403–2413.

Kim SJ, Cegelski L, Studelska DR, O'Connor RD, Mehta AK, Schaefer J. 2002. Rotational-echo double resonance characterization of vancomycin binding sites in *Staphylococcus aureus*. Biochemistry 41:6967–6977.

Kumar DM, Perez E, Cai ZY, Aoun P, Brun-Zinkernagel AM, Covey DF, Simpkins JW, Agarwal N. 2005. Role of nonfeminizing estrogen analogues in neuroprotection of rat retinal ganglion cells against glutamate-induced cytotoxicity. Free Rad Biol Med 38: 1152–1163.

Lacort M, Leal AM, Liza M, Martin C, Martinez R, Ruizlarrea MB. 1995. Protective effect of estrogens and catecholestrogens against peroxidative membrane damage in-vitro. Lipids 30:141–146.

Liu R, Yang SH, Perez E, Yi KD, Wu SS, Eberst K, Prokai L, Prokai-Tatrai K, Cai ZY, Covey DF, Day AL, Simpkins JW. 2002. Neuroprotective effects of a novel non-receptor-binding estrogen analogue: in vitro and in vivo analysis. Stroke 33:2485–2491.

Lunn WH, Farkas E. 1968. The adamantyl carbonium ion as a dehydrogenating agent, its reactions with estrone. Tetrahedron 24:6773–6776.

McDowell LM, Schaefer J. 1996. High-resolution NMR of biological solids. Curr Opin Struct Biol 6:624–629.

McDowell LM, McCarrick MA, Studelska DR, O'Connor RD, Light DR, Guilford WJ, Arnaiz D, Dallas JL, Poliks B, Schaefer J. 2003. Human Factor Xa bound amidine inhibitor conformation by double rotational-echo double-resonance nuclear magnetic resonance and molecular dynamics simulations. J Med Chem 46: 359–363.

McDowell LM, Poliks B, Studelska DR, O'Connor RD, Beusen DD, Schaefer J. 2004. Rotational-echo double-resonance NMR-restrained model of the ternary complex of 5-enolpyruvylshikimate-3-phosphate synthase. J Biomol NMR 28:11–29.

Miller CP, Jirkovsky I, Hayhurst DA, Adelman SJ. 1996. In vitro antioxidant effects of estrogens with a hindered 3-OH function on the copper-induced oxidation of low density lipoprotein. Steroids 61:305–308.

Mooradian AD. 1993. Antioxidant properties of steroids. J Steroid Biochem Mol Biol 45:509–511.

Nakamizo T, Urushitani M, Inoue R, Shinohara A, Sawada H, Honda K, Kihara T, Akaike A, Shimohama S. 2000. Protection of cultured spinal motor neurons by estradiol. Neuroreport 11:3493–3497.

O'Connor RD, Schaefer J. 2002. Relative CSA-dipolar orientation from REDOR sidebands. J Magn Reson 154:46–52.

Pauli J, van Rossum B, Forster H, de Groot HJM, Oschkinat H. 2000. Sample optimization and identification of signal patterns of amino acid side chains in 2D RFDR spectra of the α-spectrin SH3 domain. J Magn Reson 143:411–416.

Perez E, Liu R, Yang SH, Cai ZY, Covey DF, Simpkins JW. 2005. Neuroprotective effects of an estratriene analog are estrogen receptor independent in vitro and in vivo. Brain Res 1038:216–222.

Perez E, Cai ZY, Covey DF, Simpkins JW. 2006. Neuroprotective effects of estratriene analogs: structure-activity relationships and molecular optimization. Drug Dev Res 66:78–92 (this issue).

Pike CJ. 1999. Estrogen modulates neuronal Bcl-x_L expression and β-amyloid-induced apoptosis: relevance to Alzheimer's disease. J Neurochem 72:1552–1563.

Rao PN, Cessac JW, Kim HK. 1994. Preparative chemical methods for aromatization of 19-nor-Δ^4-3-oxosteroids. Steroids. 59: 621–627.

Romer W, Oettel M, Droescher P, Schwarz S. 1997a. Novel "scavestrogens" and their radical scavenging effects, iron-chelating, and total antioxidative activities: $\Delta^{8,9}$-dehydro derivatives of 17α-estradiol and 17β-estradiol. Steroids 62:304–310.

Romer W, Oettel M, Menzenbach B, Droescher P, Schwarz S. 1997b. Novel estrogens and their radical scavenging effects, iron-chelating, and total antioxidative activities: 17α-substituted analogs of $\Delta^{9(11)}$-dehydro-17 β-estradiol. Steroids 62: 688–694.

Schaefer J, McKay RA. 1999. Multi-tuned single-coil transmission line probe for nuclear magnetic resonance spectrometer, U.S. Patent 5,861,748.

Simpkins JW, Yang S-H, Liu R, Perez E, Cai ZY, Covey DF, Green PS. 2004. Estrogen-like compounds for ischemic neuroprotection. Stroke 35:2648–2651.

Simpkins JW, Yang S-H, Wen Y, Singh M. 2005. Estrogens, progestins, menopause and neurodegeneration: basic and clinical studies. Cell Mol Life Sci 62:271–280.

Smith SO, Kawakami T, Liu W, Ziliox M, Aimoto S. 2001. Helical structure of phospholamban in membrane bilayers. J Mol Biol 313:1139–1148.

Straus SK, Bremi T, Ernst RR. 1997. Side-chain conformation and dynamics in a solid peptide. J Biomol NMR 10:119–128.

Toke O, Maloy WL, Kim SJ, Blazyk J, Schaefer J. 2004a. Secondary structure and lipid contact of a peptide antibiotic in phospholipid bilayers by REDOR. Biophys J 87:662–674.

Toke O, O'Connor RD, Weldeghiorghis TK, Maloy WL, Glaser RW, Ulrich AS, Schaefer J. 2004b. Structure of $(KIAGKIA)_3$ aggregates in phospholipid bilayers by solid-state NMR. Biophys J 87:675–687.

Tong G, Pan Y, Pryor R, Wilson GE, Schaefer J. 1997. Structure and dynamics of pentaglycyl bridges in the cell walls of *Staphylococcus aureus* by ^{13}C–^{15}N REDOR NMR. Biochemistry 36: 9859–9866.

Tristram-Nagle S, Nagle JF. 2004. Lipid bilayers: thermodynamics, structure, fluctuations, and interactions. Chem Phys Lipids 127:3–14.

Weldeghiorghis TK, Schaefer J. 2003. Compensating for pulse imperfections in REDOR. J Magn Reson 165:230–236.

Wise PM, Dubal DB, Wilson ME, Rau SW. 2000. Estradiol is a neuroprotective factor in in vivo and in vitro models of brain injury. J Neurocytol 29:401–410.

Xia S, Cai ZY, Thio LL, Kim-Han JS, Dugan LL, Covey DF, Rothman SM. 2002. The estrogen receptor is not essential for all estrogen neuroprotection: new evidence from a new analog. Neurobiol Dis 9:282–293.

Yuan SS. 1982. Synthesis of 3,4-$^{13}C_2$ steroids. Steroids 39:279–289.